A Model-Predictive Control Strategy for Alleviating Voltage Collapse

Jonathon A. Martin Ian A. Hiskens

***Abstract*—Heavily loaded power systems are often susceptible to voltage collapse. The collapse process tends to evolve quickly, providing limited opportunity for operators to intervene. Therefore, a model-predictive control (MPC) scheme has been developed to alleviate line overloads and voltage collapse through strategic management of controllable resources. MPC-based corrective control builds on a system model that provides an approximate prediction of behaviour over a finite horizon. Transformer tapping plays an important role in the voltage collapse process, so MPC must incorporate an adequate model of transformer voltage regulation. The proposed MPC strategy has been demonstrated using two standard test systems, one based on the BPA network and the other on the Nordic system.**

I. Introduction

VOLTAGE control and reactive power management began receiving increased attention during the 1970s and 1980s [1]–[6]. Long-distance bulk power transfer started testing the limits of existing transmission practices and more sophisticated voltage control techniques were sought to address this challenge. Local voltage control devices were coordinated to more effectively achieve system-wide objectives. In [7], real-time optimization of generator voltage set-points, tap-changing transformers, and reactive compensation devices was applied to minimize voltage violations and system losses. Similarly, secondary voltage control schemes [8] started considering interarea interactions [9] and coordinated under-voltage load shedding [10] to achieve better performance. Nevertheless, there remained a need for more precise automatic control techniques [11].

As optimal power flow formulations began to account for both active and reactive power, the modern security-constrained economic dispatch process was born. In addition to correcting voltage violations, these algorithms started considering the economic impact of attaining a secure solution [12]. However, methods to better capture system flexibility and future behaviour continue to be opportunities for improvement.

One control technique that is well suited to handling a variety of system conditions while considering future behaviour is model-predictive control (MPC) [13], [14]. It also provides a systematic approach to resolving discrepancies arising from the use of linear models for controlling nonlinear systems. MPC uses an internal (approximate) model of the system to predict behaviour and establish an optimal control sequence. The control actions from the first step of this sequence are implemented on the actual system. Subsequent measurement of the resulting system behaviour provides the initial conditions for MPC to again predict behaviour and recalculate an optimal control sequence. The feedback inherent in the repetition of this process allows MPC to control a broad range of devices while effectively satisfying a multi-period constrained optimal power flow problem.

After demonstrating its potential in the process industry, MPC began appearing in the power systems literature to address dynamic voltage control challenges. One of the earliest investigations was presented in [15]. The method used search-based techniques and detailed nonlinear and discrete system models to determine appropriate settings for automatic voltage regulators, tap-changing transformers, and load shedding during a voltage emergency. Similar follow-up studies are also presented in [16], [17]. Since that time, subsequent works have applied techniques from MPC to address rapid voltage control in an online setting.

Trajectory sensitivity concepts have emerged as a useful basis for MPC. Under this approach, a nominal trajectory is determined for the system, and trajectory sensitivities describe (approximately) how control changes cause the system to deviate from this trajectory [18]. An open-loop voltage protection scheme, developed in [19], used trajectory sensitivities to determine a single set of control inputs which remain fixed over the entire prediction horizon. This method is adapted in [20] to operate in a closed-loop manner. In [21], trajectory sensitivities are used to identify nondisruptive load shedding controls to improve voltage stability. Automatic voltage regulator adjustment and load shedding are used as voltage controls in [22], and the trajectory sensitivity model is compared against other integration techniques. Voltage control using MPC and trajectory sensitivities is investigated in [23] with capacitor switching as the control actuator.

In addition to using trajectory sensitivities, other detailed formulations of MPC have also been used to correct voltage concerns. Instead of using search-tree solution techniques as was done in [15], [16], the authors of [24] use an interior-point method to solve a nonlinear problem formulation. However, they forego standard load and tap-changing transformer models and instead use a linear load recovery model to drive the system dynamics. While this model is somewhat inaccurate, it is sufficient to direct MPC toward secure corrective actions. This observation, that highly detailed models within MPC may be unnecessary, matches the findings of [22]. However, the models employed must sufficiently identify the key drivers of instability in order for MPC to respond appropriately.

Alternative formulations based on MPC strategies have also

This work was supported by the National Science Foundation through grant CNS-1238962.

Jonathon Martin is with GE Grid Solutions, Redmond, WA 98052, USA. Ian Hiskens is with the Department of Electrical Engineering and Computer Science, University of Michigan, Ann Arbor, MI 48109, USA (e-mail: jandrewm@umich.edu; hiskens@umich.edu).

been proposed. A protection scheme with bi-level static and dynamic optimization but which ignores the voltage recovery dynamics is proposed in [25]. In [26], loads are assumed to reach their fully recovered state and the controls selected by MPC are scaled to account for the recovery process. A distributed control process similar to MPC is described in [27].

A strength of an MPC framework is its flexibility in modeling a wide variety of system behaviour. A controller operating in real-time must be able to respond to unplanned events and accurately account for the system response in those situations. Although voltage decay and instability may occur too quickly for a human operator to intervene, automatic control strategies such as MPC have the potential to rapidly identify and avoid these situations.

The paper examines the voltage instability process and MPC's ability to correct detrimental behaviour. The voltage instability process is presented in Section II. An overview of MPC is provided in Section III and a transformer tapping model suitable for MPC implementation is discussed in Section IV. Sections V and VI discuss MPC's performance on two networks commonly used as voltage instability case studies. These demonstrations show that MPC can prevent voltage instability from occurring even in situations where a human operator would likely fail to do so. The interplay between thermal transmission limitation and load-based voltage instability is also discussed. Conclusions are provided in Section VII.

II. The Voltage Instability Process

Voltage instability describes different behaviour in different power system settings. While it may describe fast behaviour when dealing with induction motors, this work considers the slower behaviour driven by transformer tap changing and load recovery. Dynamics at the faster time scales are assumed to be secure so that the system settles back to the slower dynamic trajectory. Either way, voltage instability implies the lack of voltage stability. Voltage stability is generally defined as voltages recovering to a secure equilibrium condition following a disturbance [28]. For fast timescales, the equilibrium is described by the power flow equations with fixed taps. For slower timescales, equilibrium implies that voltage regulation changes (such as transformer tap-changing) have subsided.

The subtleties between voltage instability and other forms of instability (such as generator rotor angle instability) can be difficult to separate in faster settings. However, voltage instability on slower timescales typically is located near loads [28], [29]. As seen from the transmission network, loads are mostly voltage dependent. If the voltage magnitude drops, the power consumed by the loads will also drop. Transformers attempt to restore the voltage and therefore the power consumption of the loads. This restoration process may push the network and generators beyond their power capability limits leading to cascading outages and ultimately resulting in voltage instability [29]. Two common symptoms of voltage instability are low voltages originating near load centers and emanating into the rest of the transmission network and generators reaching their reactive power limits and losing their voltage regulation capability.

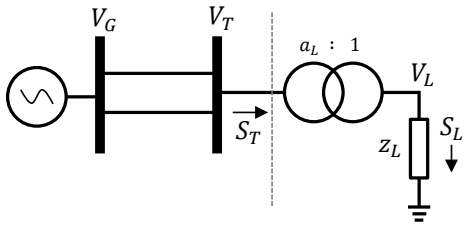

Fig. 1. Simple network demonstrating load and voltage relationships.

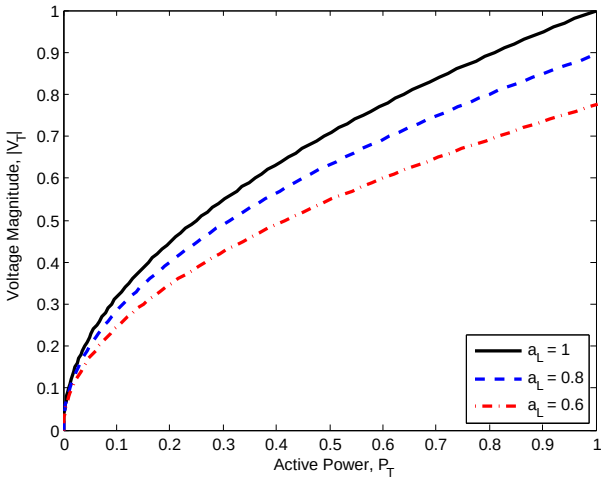

Fig. 2. The load characteristic from the system of Figure 1 is influenced by the tap ratio of the load transformer. The active power from (2) is a quadratic function of the transmission voltage magnitude. Units assume $z_L = 1$ pu.

A. Load restoration

The implications of load restoration in power system networks can be demonstrated through a simple example. Consider the network shown in Figure 1 where a generator supplies power to a load (to the right of the dashed line) through two transmission lines. The load is represented by impedance z_L, and an ideal transformer regulates the load voltage V_L by adjusting its tap position a_L. Since the transformer is ideal, the power drawn from the network S_T is equal to the power consumed by the load S_L,

$$S_T = S_L = \frac{|V_L|^2}{z_L^*}, \tag{1}$$

where z_L^* denotes the complex conjugate of z_L. Employing the transformer voltage relationship $|V_L| = |V_T|/a_L$ allows further simplification,

$$S_T = \frac{|V_T|^2}{a_L^2 z_L^*}. \tag{2}$$

Variations in the transformer tap position change the effective load impedance as seen from the transmission network. Figure 2 demonstrates the relationship between the active power drawn from the network P_T and the transmission network voltage magnitude $|V_T|$ assuming $z_L = 1$ pu. Reducing a_L increases the load on the transmission network (assuming that $|V_T|$ remains fixed as a_L changes). In the case of a low load voltage $|V_L|$, the transformer decreases its tap until the load voltage is restored to the desired level.

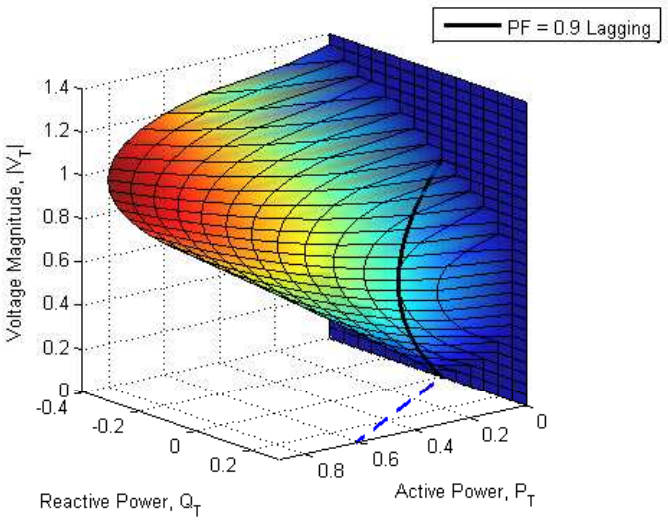

Fig. 3. The network characteristic for the system shown in Figure 1. Units assume $V_G = 1$ pu and the transmission network impedance is purely inductive with $X = 1$ pu.

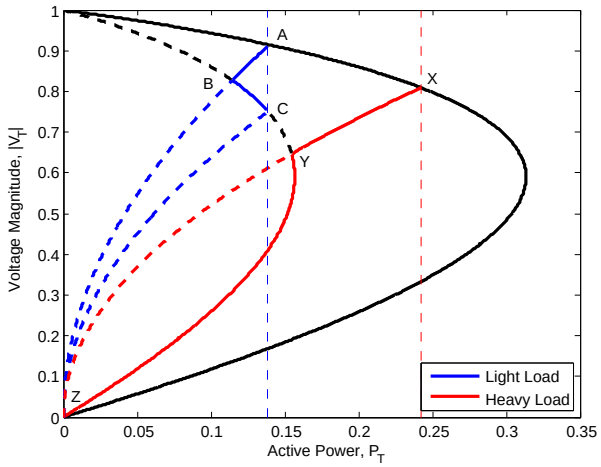

Fig. 4. Transmission network characteristic (shown in the solid black curve) for the system of Figure 1 and assuming a purely inductive network $X = 1$ pu. The load power factor is fixed at 0.9 lagging. If one of the transmission lines is lost, the transmission impedance doubles and the network characteristic is represented by the dashed black curve.

B. Network characteristic

It is also possible to determine a network characteristic describing how V_T and S_T relate to each other over a range of loading conditions. Assuming that the network from Figure 1 has a purely inductive transmission impedance $X = 1$ pu, Figure 3 shows the relationship between power and voltage. A derivation of this relationship is provided in [29].

Examining Figure 3, it becomes apparent that transmitting reactive power through the network is fundamentally difficult. In fact, the maximum reactive power that can be transmitted to the load is only a quarter of the short-circuit power at the load [29],

$$Q_T^{max} = \frac{V_G^2}{4X}. \tag{3}$$

This maximum occurs when no active power is consumed by the load ($P_T = 0$ in Figure 3). However, the active power supplied to the load can increase to any level as long as sufficient reactive compensation is provided at the load bus (e.g. Q_T becomes more negative in Figure 3). Unfortunately, significant reactive compensation will also cause unacceptable voltage rise as the load increases.

Typical operating conditions in a power system result in both active and reactive power being consumed. For example, the solid black curve in Figure 3 shows the network characteristic when the load operates at a power factor of 0.9 lagging. The ratio of active to reactive power consumption is fixed as the load level changes and is indicated by the dashed blue projection onto the power plane. The same network characteristic is represented in the $(P_T,|V_T|)$ plane by the solid black curve in Figure 4.

If one of the transmission lines is disconnected, the network impedance doubles and reduces the maximum power that can be supplied to the load. The new network characteristic is shown by the dashed black curve in Figure 4. This decrease in transmission capability implies that voltage instability becomes much more likely under heavy load conditions.

If the load transformer is set to regulate the load voltage magnitude $|V_L|$, the tap changing behaviour can degrade the transmission voltage V_T. At a long-term equilibrium condition with the load operating at its regulated voltage, the load consumes a certain amount of power (shown by the vertical dashed lines in Figure 4. It is important that this equilibrium power remains within the maximum power capability limit of the network characteristic.

The system behaviour during a contingency under light load is shown by the solid blue curve (A-B-C) in Figure 4. With both transmission lines in service and the load voltage at its set-point value, the system operates at point A. Tripping one of the transmission lines causes a rapid transition to point B along the short-term load characteristic (i.e. the impedance characteristic with a given tap ratio from Figure 2). The low load voltage at point B causes the load transformer to begin decreasing its tap until the load voltage is restored to its set-point value. This causes a slower transition from point B to point C, where the system rests at its new long-term equilibrium condition.

Under heavier load, a new long-term equilibrium condition does not exist at the desired load voltage after the loss of a transmission line. The system trajectory in this situation is shown by the solid red curve (X-Y-Z) in Figure 4. With both lines in service and the load voltage at its set-point value, the system operates at point X. The system moves rapidly to point Y when a transmission line is lost, causing a low load voltage. As the load transformer attempts to restore the load voltage by decreasing its tap, the system moves from point Y toward point Z and experiences voltage collapse. In reality, transformer tap limits would prevent the system from reaching point Z implying an equilibrium condition along the lower portion of the red curve. However, in this condition other protective relays are likely to operate and could cause further system degradation. For example, significant reactive power losses in the network would exceed the reactive power

capability of the generator and cause its voltage to also decay to unacceptably low levels.

C. Control response to voltage instability

As mentioned earlier, voltage instability is closely tied to system loading conditions. Although the light load scenario in Figure 4 reaches a new long-term equilibrium condition within the maximum transmission capability of the network, this condition may be insecure due to unacceptably low network voltages. The voltage collapse scenario under heavier load more obviously demonstrates voltage instability. In either situation, the voltage instability must be corrected by reducing the demand on the transmission network.

In the system of Figure 1, only one generation source and transmission path is available to supply the load. To reduce the demand on the network, load levels must be reduced. This can be directly accomplished by shedding load. If low load voltages are permissible, transformer tapping operations could also be blocked or the load set-point voltage reduced. Improving the load power factor by increasing reactive power compensation could also increase the capability of the network to transmit active power and supply the load. In a more realistic meshed transmission network, other generating sources would also be available and could increase their power output to reduce the loading on the strained transmission corridor.

With these control actions at its disposal, MPC must predict the system behaviour immediately following a disturbance (e.g. trajectories B-C or Y-Z in Figure 4). If insecure conditions are predicted, MPC must begin taking actions to address the situation. Transformer tap-changing tends to be the dynamic driver of this behaviour. Section IV provides details of the transformer models and their incorporation into MPC. The case studies in Sections V and VI examine the performance of these models and MPC's response to voltage instability.

III. Model-Predictive Control

The term MPC does not refer to a specific control strategy but rather to a group of strategies which utilize a process model to find a control sequence over a specified horizon by minimizing an objective function [13]. If the horizon is finite or the model imperfect, the strategy is repeated as time progresses and new information becomes available.

This work considers a finite horizon with M discrete intervals of duration T_s. At a given discrete time instance l, the MPC process is initiated to determine the behaviour of some states[1], $x[k|l]$ for $k \in \{1, \ldots, M\}$, driven by controls, $u[k|l]$ for $k \in \{0, \ldots, M-1\}$. The notation $x[k|l]$ represents the modeled states at time $l+k$ given an initiation of the model at time l. The first control in the sequence, $u[0|l]$, is implemented on the physical system. When new system measurements for the states become available at the next discrete time instance $l+1$, the process is repeated to find the new control sequence, $u[k|l+1]$ for $k \in \{0, \ldots, M-1\}$. Since the MPC process is repeated at every discrete time instance, the notation of l becomes somewhat unnecessary and cumbersome as it is typically evident from context. In this work, the notation $u[k]$ will be used as a shorthand for $u[k|l]$.

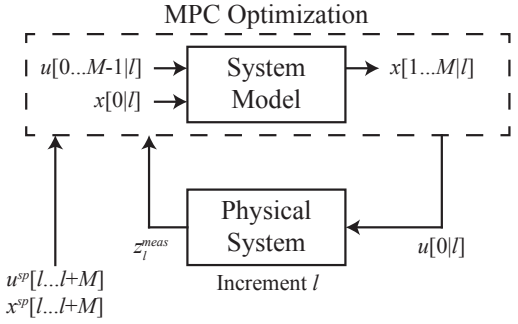

Fig. 5. Overview of MPC strategy.

The proposed MPC strategy repeatedly solves a form of multi-period optimal power flow that considers slower dynamic processes associated with transmission line conductor temperature, transformer tap-changing, energy storage state-of-charge, and ramp-limited generation. For such processes, a controller response rate on the order of one minute is sufficient. Sub-second voltage and generator transients are significantly faster than the time constants of these slower processes. It is assumed fast transients are stabilized by standard closed-loop controls (e.g. generator automatic voltage regulators and power system stabilizers) and are ignored in the MPC model.

Figure 5 outlines the MPC control strategy. At time l, all measurements necessary to model the network, z_l^{meas}, are provided to the controller. These measurements include voltages, generation, storage state-of-charge, device operating states, network configuration, transmission line temperatures, and the most recent load and renewable forecasts. This information is obtained from SCADA/PMU measurements and state estimation[2], and determines the initial value of the system state $x[0|l]$. MPC then builds an optimization problem to determine a control sequence $u[0 \ldots M-1|l]$ over a horizon of M time-steps while considering its effects on the states $x[1 \ldots M|l]$ using a model of the system. The controls are selected to track scheduled set-point values[3] for both the controls $u^{sp}[l \ldots l+M-1]$ and states $x^{sp}[l+1 \ldots l+M]$ over the prediction horizon. Once an optimal control sequence is identified, the controls from the first step in the sequence, $u[0|l]$, are applied to the physical system in a step-wise manner with constant step-width T_s, giving $u(t) := u[0|l]$ for $t \in [(l)T_s, (l+1)T_s)$. The physical system responds to the controls as time advances from l to $l+1$, and the process repeats when new system measurements z_{l+1}^{meas} become available.

The MPC strategy extends naturally to power system applications due to its compatibility with present economic dispatch techniques. The MPC formulation presented in this work operates every minute whereas traditional security-constrained economic dispatch programs operate every five minutes [30],

[1]It is assumed that states are observable and can be measured.

[2]The time delays inherent in SCADA and state estimation (less than 60 seconds [30]) can be ignored as they are small relative to the time constants of the dynamic processes considered in this MPC formulation.

[3]These scheduled values are typically established by economic dispatch.

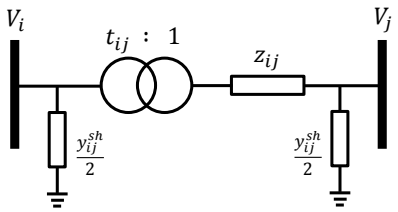

Fig. 6. The Unified Branch Model allows both transformers and transmission lines to be described within a single framework.

[31]. In the PJM and NYISO networks, severe overloads exceeding the load dump or short-term emergency ratings, respectively, must be resolved within five minutes [30], [32] to prevent tripping of a transmission line which can further exacerbate the problem. MPC identifies an optimal response within this time-frame while considering future effects of the control actions and minimizing deviations from the economic dispatch. In this way, the proposed controller assumes the role of a system operator responding to thermal rating and voltage magnitude concerns in real time while seeking to maintain, as best possible, the economic schedule.

IV. Transformer voltage regulation

Many transformers are equipped to change their tap settings (turns ratio) while operating under load, enabling them to regulate voltages across the network as loading patterns change. These devices are referred to as *load tap changers* (LTCs). If an LTC is set to automatically regulate voltage or power flow, the local feedback control process introduces dynamics that can influence behaviour across the network.

Modern power dispatch processes coordinate these local control strategies to maximize the overall system benefit and avoid unstable operation. Voltage regulating transformers primarily interact with generator voltage regulators and reactive power compensation devices such as shunt capacitors or reactors. Without proper intervention during emergencies, the interaction of the control dynamics can exacerbate the situation and lead toward system collapse.

This section describes how LTC dynamics are incorporated into MPC's internal model. Though approximate, the proposed model sufficiently captures the primary dynamic behaviour and enables MPC to identify appropriate control actions during emergency situations.

A. Unified branch model

A commonly applied framework for modeling transmission networks is the Unified Branch Model, which is shown in Figure 6. This model incorporates both transmission lines and transformers into the network description and is discussed in [33]. An ideal transformer with complex tap ratio $t_{ij} = a_{ij}\angle\psi_{ij}$ is connected in series to complex impedance z_{ij}. Any shunt admittance y_{ij}^{sh} is split evenly and lumped at the two end buses.

If the branch models a transmission line, the ideal transformer is ignored ($t_{ij} = 1$), and the series impedance and shunt admittance tend to be nonzero. If the branch models a transformer, the tap ratio will vary around 1, and the shunt admittance will tend to be zero. The series impedance may be purely imaginary if resistive effects in the transformer windings are ignored, but this is not generally the case. If the transformer is equipped with a voltage regulator, it will regulate V_j by adjusting the magnitude of t_{ij}.

Transformers may also be configured to regulate the power flow on branch ij. In this case, the power entering the branch from bus i is monitored. To regulate reactive power, the magnitude of t_{ij} is adjusted. To regulate active power, the angle of t_{ij} is adjusted.

B. Transformer tap-changing dynamics

Within the realm of power system dynamics, regulating LTCs operate slowly and in a discrete manner. Typically, they are designed to raise and lower their tap settings by $\pm 10\%$ from the neutral position over 32 additional positions. This produces individual step changes of 5/8% or 0.00625 pu. The step change happens very quickly to minimize the current interruption and is modeled as instantaneous, but mechanical switching mechanisms typically require several seconds between subsequent tapping operations.

Because regulation happens through discrete changes, a deadband d is defined around the reference target to avoid hunting (oscillatory) operation. This deadband is sized larger than the change in the regulated quantity resulting from a single tap operation. For example when regulating voltage, a tap operation typically produces an equivalently sized change in voltage magnitude (about 0.00625 pu). A common voltage deadband is specified as ± 0.01 pu. For the remainder of this discussion, transformer dynamics will be described with voltage as the regulated quantity since this is the most common configuration. The control dynamics are very similar when active or reactive power flow is regulated and these will be summarized as well when the internal model of MPC is presented in Section IV-C.

Intentional delays in addition to the mechanical delay between tapping operations are also built into the regulator control logic. Large disturbances in the network can cause voltage deviations that require several seconds to subside. Without a time delay, such temporary deviations could cause transformers to unnecessarily adjust their tap positions. This spurious behaviour would increase wear on the device and shorten its lifespan. These effects can be avoided by intentionally delaying tapping operation.

Similarly, transmission networks typically have several layers of regulating transformers between generators and loads. Tap changes at one layer will influence the voltages at the other layers requiring coordination between the timescales of operation at different layers. For example, LTCs in the higher voltage transmission network may be set to operate more quickly than those in lower voltage sub-transmission networks. Changing the voltage in the transmission network tends to produce a similar change in the sub-transmission network. If both portions of the network have low voltages following a disturbance, increasing the transmission level voltage first may remove the deadband violation at the sub-transmission

level as well and result in fewer tapping operations overall. Alternatively, a poorly coordinated system can produce oscillatory transformer behaviour if tap changes at one layer push voltages at another layer outside their deadbands [34]. Time delays and deadbands are typically set during system design and are modeled as fixed quantities in this analysis.

1) Discrete model of transformer tap-changing: The intentional delay between tapping operations can be a fixed quantity or vary with the severity of the deadband violation. In this way, the time between tapping operations is not an independent variable. A discrete time index s can be defined to increment whenever a tap change operation occurs. If a deadband violation is detected, an internal counter T_{vio} starts tracking the time over which the deadband violation is sustained. If it persists long enough to exceed the intentional delay T_d, a tap change operation occurs and $s \to s+1$.

To account for the various intentional delay settings, a composite formulation can be used [29],

$$T_d = T_m + T_f + T_p \frac{d}{|V - V^{ref}|}. \tag{4}$$

Here, T_m is the mechanical delay required by the switching mechanism, T_f is any additional fixed delay specification, and T_p parameterizes the proportional delay term which varies with the severity of the deadband violation. Large deviations in the regulated voltage V away from its reference target value V^{ref} result in shorter delays between tapping operations.

After a deadband violation is sustained past the intentional delay ($T_{vio} > T_d$), a tap change is initiated. Voltage regulating transformers adjust their tap magnitude a by step size a^{stp} using the logic [29],

$$a_{s+1} = \begin{cases} a_s + a^{stp}, & \text{if } V > V^{ref} + d \text{ and } a_s < a^{max} \\ a_s - a^{stp}, & \text{if } V < V^{ref} - d \text{ and } a_s > a^{min} \\ a_s, & \text{otherwise.} \end{cases} \tag{5}$$

This ensures that the tap remains within its upper and lower limits, a^{max} and a^{min} respectively. The tapping logic in (5) is appropriate for regulating the voltage at bus j in the circuit orientation shown in Figure 6. In order to regulate V_j, tap changes occur on the opposite side of the transformer closer to bus i. Therefore, increasing the tap magnitude a_{ij} will reduce voltage magnitude V_j and vice versa. If the regulated voltage is within its deadband or the tap is against a limit, a tap change will not occur.

The duration of T_d can vary quite significantly across different systems and in different parts of a single system. However, it is fairly common for the delay to fall in the range of $30 - 120$ seconds [28], [29]. Sometimes a distinction will be made between the delay on the first tapping operation in a sequence and subsequent tapping operations. This is classified as a "sequential mode" of operation [29]. For instance the delay on the first operation may be defined as in (4), but subsequent delays may set $T_f = T_p = 0$ to permit faster operation in response to large voltage deviations. When no distinction is made in the delay setting throughout the tapping sequence, it is referred to as a "non-sequential mode" of operation [29]. Though faster operation of transformers allows deadband violations to be resolved more quickly under normal conditions, it also reduces the intervention time available during voltage collapse conditions.

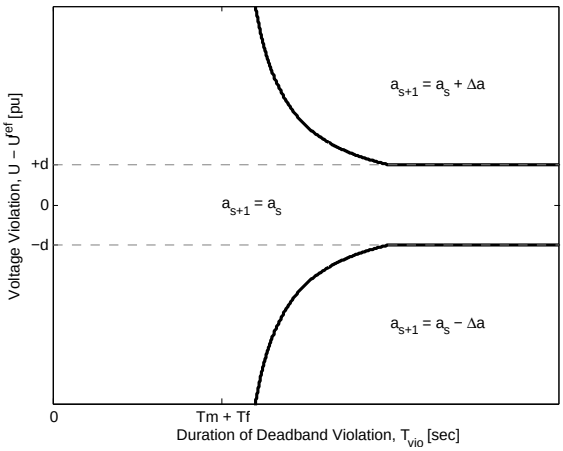

Fig. 7. Transformer tap-changing dynamics (5) are discrete and depend on deadband and delay specifications. The delay T_d from (4) is shown by the solid black curves and bounds the upper-right and lower-right regions where tap changes occur. The dashed gray lines denote the voltage deadband. If a voltage violation occurs outside the deadband, T_{vio} begins increasing from 0 until it reaches T_d, initiating a tap change. If the voltage returns to within the deadband while $T_{vio} < T_d$, T_{vio} resets to 0.

The transformer dynamics specified by (4) and (5) are highly nonlinear due to the variable time delay and discrete tap transitions. Figure 7 summarizes these dynamics. The delay T_d from (4) is shown in the solid black curves and assumes nonzero values for the fixed ($T_m + T_f$) and proportional (T_p) time constants. These curves separate the three unique regions in (5). When transitioning from the central region to the upper-right or lower-right regions, a discrete tap change occurs. If the proportional time constant T_p is reduced to zero, the upper-right and lower-right regions become rectangular and are bounded on the left by $T_m + T_f$ and horizontally by the deadband (shown in the dashed gray lines).

If a voltage violation occurs outside the deadband, the timer T_{vio} begins increasing from zero (i.e. moving from left to right in Figure 7). If the voltage violation remains outside the deadband, T_{vio} continues to increase until it reaches one of the T_d curves and a tap change occurs. The timer T_{vio} resets to zero if the voltage violation decreases in magnitude and moves back to within the deadband while $T_{vio} < T_d$ or once a tap change has occurred.

2) Continuous model of transformer tap-changing: To be applied within MPC, the transformer dynamics must be approximated by a linear formulation with continuous variables. A straightforward model is presented in [29] which ignores the deadband and fixed time constants, and treats the transformer tap position as a continuous variable. This results in the dynamic relationship,

$$\dot{a} = \frac{1}{T_{dl}} \left(V - V^{ref} \right), \tag{6a}$$

$$a^{min} \leq a \leq a^{max}. \tag{6b}$$

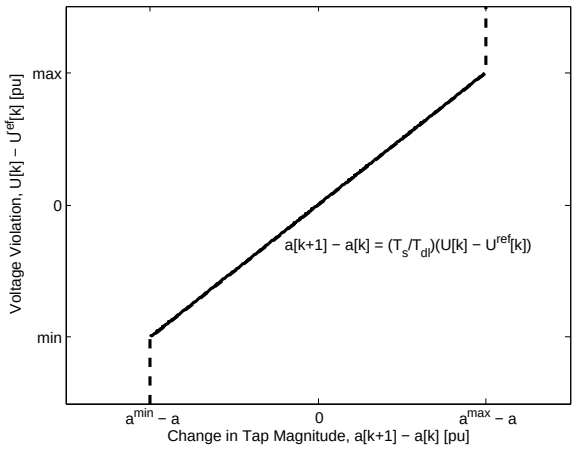

Fig. 8. Transformer tap change dynamics within MPC (9) are continuous and linear. The linear delay constant T_{dl} is given by (8).

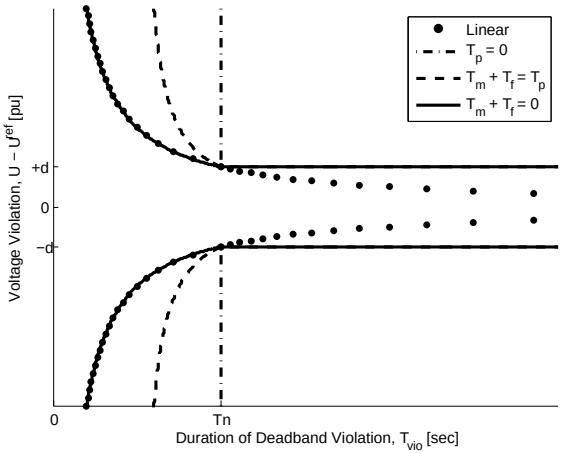

Fig. 9. Transformer tap-changing dynamics under both the discrete and linear models. The curves represent the tap step under the discrete model with different delay characteristics. The linear model assumes the tap changes continuously from the origin, and the dots show where it predicts the tap change is equal to the tap-step size $|\dot{a}T_{vio}| = a^{stp}$.

This turns the tap magnitude a into an integrator of the voltage error $V - V^{ref}$. The linear delay constant T_{dl} is given by

$$T_{dl} = \frac{T_p d}{a^{stp}}. \tag{7}$$

The fixed delay constants T_m and T_f are assumed to be zero under this formulation [29].

It is possible, however, that the transformer delay is only specified with fixed delay constants, i.e. $T_p = 0$. When this occurs the model from [29] is ill-defined and the gain in (6a) goes to infinity. To resolve this condition, the linear delay constant is redefined here as

$$T_{dl} = \frac{(T_m + T_f + T_p)\, d}{a^{stp}}. \tag{8}$$

Substituting (8) into (6) gives

$$\dot{a} = \frac{a^{stp}\left(V - V^{ref}\right)}{d\left(T_m + T_f + T_p\right)}, \tag{9a}$$

$$a^{min} \leq a \leq a^{max}. \tag{9b}$$

The tap changing dynamics given by (9) are applied within MPC to approximate the true discrete behaviour specified by (4) and (5). Instead of changing in discrete steps, the tap is assumed to vary continuously between its minimum and maximum values. Implementing (9a) within the discrete time framework of MPC implies that any voltage deviation will be sustained for the entire duration of each time-step T_s. Therefore, the change in tap from one time-step to the next can be defined as,

$$\Delta a[k+1] - \Delta a[k] = \dot{a}[k] T_s = \frac{T_s}{T_{dl}} \left(V[k] - V^{ref}[k]\right). \tag{10}$$

Figure 8 shows that continuous changes in the tap position result from voltage deviations within the linear dynamics (10). However, enforcing the tap limits (9b) introduces switching into the model (evidenced by the knee points in the curve in Figure 8). MPC must always comply with the tap limits (9b). Therefore, with V^{ref} fixed, MPC may be forced to take drastic control actions to alleviate voltage fluctuations that would drive operation beyond the solid linear portion of the curve. Enforcing transformer limits through such aggressive behaviour is unrealistic. In practice, operators are not concerned if a transformer reaches its tap limit. Although this condition might be a signal that the system is stressed, it does not threaten the safety of the network. In fact, it may help to slow some voltage collapse situations by preventing voltage dependent loads from recovering completely.

A straightforward method of ensuring that MPC can satisfy the linear tap change dynamics while enforcing tap limits is to allow the reference voltage V^{ref} to vary. Figure 8 shows how encountering a tap limit induces an artificial limit on the voltage error $V - V^{ref}$. Adjusting V^{ref} allows the voltage V to fluctuate arbitrarily while keeping the voltage error within its linear range.

The definition of T_{dl} given in (8) does not make any distinction between fixed and proportional time delays. Instead, it treats all delays as proportional which introduces some error into the model. Figure 9 shows the tap change under both the discrete model of (4) and (5) and the linear model of (9) for a variety of time delay characteristics. The sum of the delay constants is equal for each curve to provide a normalized comparison, $T_n = T_m + T_f + T_p$.

The curves in Figure 9 show where the discrete model predicts the tap step will occur. When only fixed delays are modeled, $T_p = 0$, the delay is insensitive to the size of the voltage violation. As the delay shifts toward a proportional characteristic, $T_m + T_f = 0$, tap changes occur more rapidly for large voltage violations.

The linear model assumes that the tap changes continuously depending on the magnitude and duration of the voltage violation. The dots in Figure 9 show where the linear model predicts the tap change is equal to the tap-step size, $|\dot{a}T_{vio}| = a^{stp}$. If the delay characteristic is purely proportional, the linear and discrete models are fairly similar. Greater discrepancies arise when the delay characteristic is actually fixed. In this situation, the linear model predicts larger tap changes than the discrete

model for the same duration of the voltage violation.

This overprediction of tap changes within the linear model of MPC has different implications depending on the operating situation. Under normal operating conditions, the tap changes restore system voltages to their desired levels. Overprediction of the tap change implies that this restoration will occur quickly and causes MPC to avoid taking additional control actions to restore voltages. Alternatively, during heavy load conditions, tap changing can cause undesirable voltage behaviour. Overprediction of the tap changes in this scenario causes MPC to select more aggressive corrective measures than may be necessary to prevent the tap changing from driving the system unstable.

3) Numerical stability of transformer dynamics in MPC: The step-size T_s of MPC must be chosen small enough to ensure numerical stability of the transformer model. In a linear system with $\dot{a} = \lambda a$, where λ approximates the eigenvalues of the system, the system is stable as long as $\mathrm{Real}(\lambda) < 0$. When using Euler discretization, the system dynamics are represented,

$$a[k+1] = a[k] + T_s \lambda a[k]. \tag{11}$$

This can be condensed to

$$a[k+1] = (1 + T_s\lambda)^{k+1}\, a[0]. \tag{12}$$

In order for this system to be stable, it must approach zero as k approaches infinity. This requires

$$|1 + T_s\lambda| < 1 \Leftrightarrow -1 < 1 + T_s\lambda < 1. \tag{13}$$

From this, the choice of T_s must satisfy two requirements:

$$T_s > 0, \tag{14a}$$

$$T_s < \frac{-2}{\lambda}. \tag{14b}$$

Assuming λ is negative, the conditions of (14) require that T_s be a small positive number for the numerical stability to match the underlying dynamic stability.

The tap dynamics of (10) are expressed in terms of voltage magnitude instead of the current tap position. To confirm numerical stability properties, (10) must be rearranged so that the tap position appears explicitly as in (11). The voltage behaviour within MPC is driven by (approximate) linear power flow equations. Rearranging these equations allows voltage magnitudes to be expressed in terms of transformer behaviour and power injections across the network. Substituting for $V[k]$ in (10) gives,

$$\Delta a[k+1] = \Delta a[k] + \frac{T_s}{T_{dl}}\Big(\big[\frac{dV}{da}\Delta a[k] + \frac{dV}{dp_G}\Delta p_G[k] + \dots \big] + V^{meas} - V^{ref}[k] \Big). \tag{15}$$

Grouping the coefficients of $\Delta a[k]$ in (15) allows an equivalent condition to that of (13) to be defined:

$$-1 < 1 + \frac{T_s}{T_{dl}}\frac{dV}{da} < 1. \tag{16}$$

Given that dV/da is negative, this implies that T_s must be chosen to satisfy,

$$T_s > 0, \tag{17a}$$

$$T_s < \frac{-2T_{dl}}{dV/da}. \tag{17b}$$

As system conditions change, the sensitivity dV/da will also change. Under normal conditions, this sensitivity is around -1. However, in a voltage collapse situation the sensitivity approaches zero [29]. This loss of sensitivity effectively relaxes the constraint of (17b). Therefore, selecting $T_s < 2T_{dl}$ will tend to satisfy numerical stability requirements for transformer models under all operating conditions. As mentioned previously, typical values for a^{stp}, d, and $T_m + T_f + T_p$ are 0.00625 pu, 0.01 pu, and $30 - 120$ seconds, respectively. This causes T_{dl} to fall in the range $48 - 192$ seconds, enabling the choice of $T_s = 60$ seconds for the MPC time-step.

C. Transformer constraints

The set of constraints describing the behaviour of a voltage regulating transformer with the branch configuration shown in Figure 6 are

$$\Delta a_{ij}[k+1] = \Delta a_{ij}[k] + \frac{a_{ij}^{stp} T_s}{d_{ij}(T_{m,ij} + T_{f,ij} + T_{p,ij})} \times \big(\Delta V_j[k] + V_j^{meas} - V_{ij}^{ref}[k]\big), \tag{18a}$$

$$\Delta a_{ij}[0] = 0, \tag{18b}$$

$$a_{ij}^{min} \le \Delta a_{ij}[k+1] + a_{ij}^{meas} \le a_{ij}^{max}, \tag{18c}$$

for $k \in \{0, \dots, M-1\}$. The tap magnitude a_{ij} is driven by the dynamics of (18a) with Δa_{ij} describing changes from the measured tap magnitude at the start of the prediction horizon. MPC has the ability to influence this behaviour by adjusting the voltage magnitude reference V_{ij}^{ref}. Changes to the reference are penalized quadratically in the objective function. The tap position is initialized to the measured value using (18b). Equation (18c) ensures that the tap magnitude remains within its lower and upper limits.

If the transformer is configured to regulate its reactive power flow, the voltage terms in (18) are replaced with reactive power flow terms:

$$\Delta a_{ij}[k+1] = \Delta a_{ij}[k] + \frac{a_{ij}^{stp} T_s}{d_{ij}(T_{m,ij} + T_{f,ij} + T_{p,ij})} \times \big(\Delta q_{ij}[k] + q_{ij}^{meas} - q_{ij}^{ref}[k]\big), \tag{19a}$$

$$\Delta a_{ij}[0] = 0, \tag{19b}$$

$$a_{ij}^{min} \le \Delta a_{ij}[k+1] + a_{ij}^{meas} \le a_{ij}^{max}, \tag{19c}$$

$$\Delta q_{ij}[k] = \frac{\partial q_{ij}}{\partial a_{ij}}\Delta a_{ij}[k] + \frac{\partial q_{ij}}{\partial U_i}\Delta U_i[k] + \frac{\partial q_{ij}}{\partial U_j}\Delta U_j[k], \tag{19d}$$

for $k \in \{0, \dots, M-1\}$. Again, the tap magnitude a_{ij} is driven by the dynamics of (19a), and MPC has the ability to influence this behaviour by adjusting the reactive power flow reference q_{ij}^{ref}. Any changes to q_{ij}^{ref} are quadratically penalized in the objective function. The tap position is initialized by (19b), and (19c) ensures that the tap magnitude remains within its

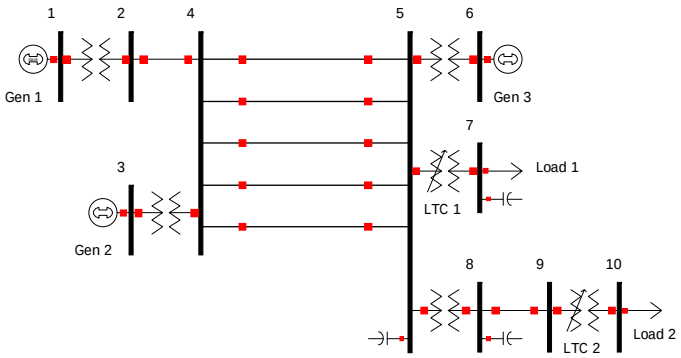

Fig. 10. Small equivalent BPA network.

lower and upper limits. The reactive power flow q_{ij} through the transformer is defined by (19d) where the notation ΔU denotes a condensed representation of $[\Delta\delta \;\; \Delta V]^\top$.

A similar set of constraints is necessary for transformers regulating their active power flow:

$$\Delta\psi_{ij}[k+1] = \Delta\psi_{ij}[k] + \frac{\psi_{ij}^{stp} T_s}{d_{ij}(T_{m,ij} + T_{f,ij} + T_{p,ij})} \times \big(\Delta p_{ij}[k] + p_{ij}^{meas} - p_{ij}^{ref}[k]\big), \quad (20a)$$

$$\Delta\psi_{ij}[0] = 0, \quad (20b)$$

$$\psi_{ij}^{min} \leq \Delta\psi_{ij}[k+1] + \psi_{ij}^{meas} \leq \psi_{ij}^{max}, \quad (20c)$$

$$\Delta p_{ij}[k] = \frac{\partial p_{ij}}{\partial \psi_{ij}} \Delta\psi_{ij}[k] + \frac{\partial p_{ij}}{\partial U_i} \Delta U_i[k] + \frac{\partial p_{ij}}{\partial U_j} \Delta U_j[k], \quad (20d)$$

for $k \in \{0, \ldots, M-1\}$. Here, the phase angle of the transformer tap ψ_{ij} is driven by the dynamics of (20a), and MPC can influence this behaviour by adjusting the active power flow reference p_{ij}^{ref}. Changes to the reference are quadratically penalized in the objective function. The tap angle is initialized by (20b) and limits are enforced by (20c). The active power flow p_{ij} through the transformer is defined by (20d).

V. BPA Network

A small equivalent network developed by *Bonneville Power Administration* (BPA) offers useful insights into MPC's ability to correct voltage instability. The layout of this network is shown in Figure 10. Five high voltage transmission lines connect generation on the left to two loads partially offset by a local generator on the right. The system is loaded heavily so that tripping one of the high voltage transmission lines initiates a voltage instability sequence. A description of the network is provided in [28], but the relevant parameters used in this work are summarized here for completeness.

A. BPA network description

The general parameters for each bus in the BPA network are given in Table I. The nominal operating voltages are shown in the second column. The power ratings of the shunt capacitors at nominal voltage are given in the third column. The fourth and fifth columns specify the acceptable voltage ranges. Note that buses with generators have their voltage ranges fixed to the set-point voltage of the generator.

TABLE I
BPA network bus parameters

Bus	Nom. Volt. [kV]	Shunt Cap. [MVAr]	Min. Volt. [pu]	Max. Volt. [pu]
1	13.8	0	0.98	0.98
2	500	0	1	1.15
3	13.8	0	0.964	0.964
4	500	0	1	1.15
5	500	868	1	1.15
6	13.8	0	0.972	0.972
7	13.8	1500	0.9	1.1
8	115	300	0.9	1.1
9	115	0	0.9	1.1
10	13.8	0	0.9	1.1

TABLE II
BPA network branch parameters

Branch	Type	From	To	R [pu]	X [pu]	B [pu]	Tap [pu]
1	Xfrmr	1	2	0	0.002333	0	0.8857
2	Line	2	4	0	0.004	0	1
3	Xfrmr	3	4	0	0.005249	0	0.8857
4-8	Line	4	5	0.0015	0.0288	2.346	1
9	Xfrmr	5	6	0	0.005718	0	1.1082
10	LTC	5	7	0	0.003	0	-
11	Xfmr	5	8	0	0.003	0	1.0594
12	Line	8	9	0.000909	0.00303	0	1
13	LTC	9	10	0	0.001	0	-

Table II gives the branch parameters. The second column states the branch types: 'Xfrmr' references a fixed tap transformer, 'Line' references an overhead transmission line, and 'LTC' references a tap changing transformer which regulates its To bus voltage. Columns three and four provide the bus connections. Columns five and six give the series resistance and reactance, respectively. Column seven states the shunt susceptance. Finally, column eight gives the tap ratio. The tap ratios are not specified for the tap changing transformers since they vary with time. Thermal ratings are assumed to be sufficiently large and are ignored.

The voltage regulation characteristics for the tap changing transformers are given as follows. LTC 1 regulates its voltage between 0.99 and 1.01 pu by adjusting its tap between 1 and 1.1 pu with step size 0.003125 pu. It is set to operate non-sequentially with a fixed delay of 60 seconds. LTC 2 regulates its voltage between 0.99 and 1.01 pu by adjusting its tap between 0.9 and 1.1 pu with step size 0.00625 pu. It is set to operate sequentially with an initial fixed delay of 60 seconds and a subsequent fixed delay of 5 seconds.

The generators in Figure 10 regulate their terminal voltages and operate within a rectangular power capability region. Generators 1 through 3 can produce active power up to 50 pu, 22 pu, and 16 pu respectively on a 100 MVA system power base. Respectively, they can absorb reactive power up to 20 pu, 2 pu, and 2 pu and produce reactive power up to 20 pu, 7.25 pu, and 7 pu. Generator 1 operates as the slack generator and approximates a large remote system. Generator 2 is dispatched to produce active power at 15 pu, and generator 3 is dispatched at 10.94 pu. Output ramp rate limits on the generators are ignored.

TABLE III
MPC OBJECTIVE COEFFICIENTS FOR HEAVY BPA LOAD

Term	Use Voltage	Use Power
p_{Gn}	100	1
Δp_{Gn}	1	1
q_{Gn}	1	1
p_{Dn}^{red}	1,000	10
V_n^+, V_n^-	1	100
V_{ij}^{ref}	1	100
a_{ij}	0.01	0.01

The load power levels will be specified for the case studies in the following sections. Load 1 represents an industrial load connected directly to the transmission network with a constant power characteristic for its active power and constant current for its reactive power. At steady-state it operates at a power factor of 0.8575 lagging. Load 2 represents a mixture of residential and commercial loads connected at the sub-transmission level. It operates at unity power factor with its active power split evenly between constant power and constant impedance characteristics.

B. Contingency under heavy load

Tripping one of the high voltage transmission lines between buses 4 and 5 during heavy load causes a voltage instability event. Losing the transmission line significantly increases the reactive power losses and causes the voltage in the load area to drop. The voltage dependent portions of the loads decrease slightly, but the tap changing transformers begin to restore the load voltages. This restoration exceeds the reactive power capability of generator 3 and eventually drives the system unstable. The instability is identified by a lack of convergence in the power flow.

For this test case, load 1 demands $30 + \mathbf{j}18$ pu and load 2 demands 35 pu at nominal voltage. The loads remain at these nominal levels over the entirety of the scenario (though the actual power drawn varies with the voltage). The system operates with all lines in service for five minutes. At minute five, one of the interarea transmission lines trips offline. Low voltage at bus 6 causes MPC to begin operating. The pre-contingency system conditions are used as the reference trajectory for MPC. The prediction horizon length is set to $M = 11$, and the period duration is $T_s = 1$ minute.

MPC can be tuned to emphasize certain types of controls. For instance, adjusting voltage settings may be preferable to changing the power dispatch. By assigning heavier objective penalties to changes in power, MPC will rely less on these controls. The objective coefficients emphasizing voltage control are given in the second column of Table III.

Key system quantities are shown in Figure 11. The '$*$' markers show the behaviour when MPC is not operating. The '$\circ$' markers show the behaviour under MPC's control. Without intervention, collapse occurs before measurements become available at minute 7 due to rapid tap-changing on LTC 2.

The initial voltage drop in Figure 11a is quickly restored by MPC. Raising the voltage reduces the reactive power losses on the transmission lines and increases the reactive power

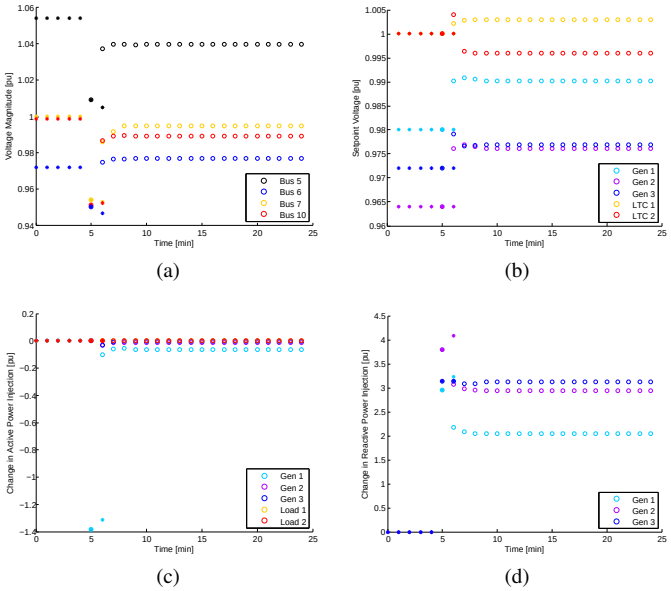

Fig. 11. Conditions during a contingency at minute 5 under heavy load when voltage control is emphasized. Behaviour with and without MPC intervention is shown by '$\circ$' and '$*$', respectively. Changes in power are with respect to the conditions at time 0. (a) Voltage magnitudes drop sharply after losing a transmission line but are restored by MPC. (b) MPC increases voltage set-points to reduce reactive power losses and better utilize shunt capacitors. (c) Active power remains mostly constant, and MPC returns the slack generator to its pre-contingency dispatch. (d) Reactive power requirements decrease as voltages recover.

support available from the shunt capacitors. Voltage set-point adjustments are inexpensive, and Figure 11b shows how MPC significantly raises the voltages at generators 1 and 2 and slightly adjusts settings in the load area.

Active power controls remain fairly constant at their pre-contingency dispatches in Figure 11c due to the high objective cost of deviations. The reactive power required from generator 3 in Figure 11d remains consistent at its reactive power limit following the contingency. The reactive requirements from generators 1 and 2 decrease between minutes 5 and 6 as the reactive power losses decrease in response to higher voltages.

This example demonstrates the importance of a coordinated voltage control strategy. Without intervention, the LTCs act as the primary drivers of load restoration, but simultaneously lower the transmission voltages and drain generator reactive power reserves. However, MPC recognizes a solution that may not be immediately obvious to an operator and requests that all generators increase their voltage set-points. Normally, increasing the voltage would require the generators to increase their reactive power outputs, even though they are already near their limits. In this case, however, because of the heavy loading on the transmission network, raising voltages reduces reactive power losses and hence reduces the reactive power output of the generators. (This is similar to the situation studies in [35].) This atypical behaviour is apparent through MPC computations, but would likely remain unnoticed using intuitive operating practices.

Alternatively, MPC can also be tuned to emphasize power adjustment and maintain the network voltage settings. The

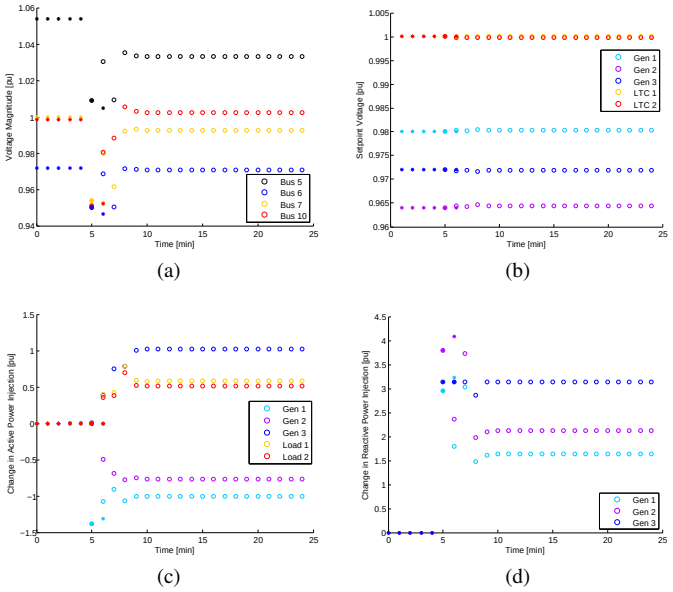

Fig. 12. Conditions during a contingency at minute 5 under heavy load when power control is emphasized. Behaviour with and without MPC intervention is shown by '$\circ$' and '$*$', respectively. Changes in power are with respect to the conditions at time 0. (a) Voltage magnitudes drop sharply after losing a transmission line and rapid tap-changing not predicted by MPC causes deterioration at minute 7 before being resolved. (b) MPC avoids adjusting voltage set-points on generators and LTCs due to cost. (c) Active power generation is shifted from the remote area to the load area, and demand response is enacted. (d) Initially large reactive power requirements are reduced as interarea transmission is relieved due to the redispatch of active power and restoration of shunt capacitor voltage.

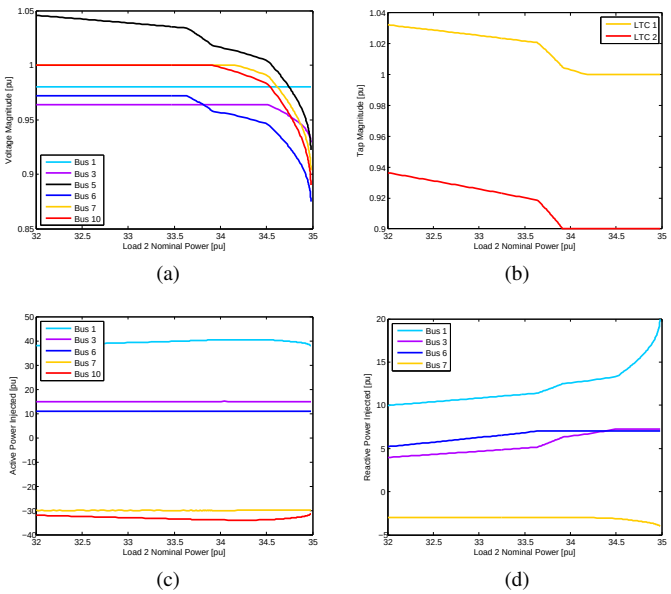

Fig. 13. Behaviour of the BPA network with one of the high voltage transmission lines removed and load 2 experiencing a slow ramp. (a) Voltages collapse quickly as the load approaches its maximum nominal value of 34.98 pu. (b) Tap changing transformers reach their limits as load increases. (c) Maximum power delivered to load 2 is 33.97 pu at nominal demand 34.19 pu. (d) Reactive power requirements increase sharply as the system approaches its loading limit.

objective coefficients emphasizing power controls are shown in the third column of Table III. The same contingency scenario is tested with these objective weights guiding MPC decisions.

Figure 12a shows the voltage behaviour when power adjustments are emphasized over voltage changes. Voltages drop sharply when the transmission line is lost at minute 5. MPC is able to partially restore the voltages by minute 6, but the voltage at bus 10 remains outside the deadband of the LTC. This initiates a rapid tap changing sequence on LTC 2 between minutes 6 and 7. The faster sequential operation is not modeled within MPC and is not predicted by the controller. This causes voltages to drop again at minute 7 (except at bus 10) and LTC 2 reaches its lower tap limit. MPC is then able to restore the voltages by minute 8. The voltage set-points in Figure 12b remain unchanged due to the high objective cost of adjustments.

Active power production is shifted from generator 2 to generator 3 and demand response is enacted on both loads in Figure 12c. This reduces the strain on the transmission network while maintaining the voltage set-points at their scheduled values. Reducing the transmission loading and restoring the load area voltage also decreases the amount of reactive power required from generators 1 and 2 in Figure 12d.

Both line trip scenarios demonstrate MPC's ability to detect and respond appropriately to sudden low network voltages. MPC is able to safely guide the system through significant disturbances, correcting situations that would likely be unavoidable for human operators.

C. *Load pickup with contingency*

Voltage instability can also arise during periods of sustained load buildup. Consider the BPA network with one of the transmission lines between buses 4 and 5 removed from service. At moderate loading levels, the network is able to operate without any limit violations. However, if load 2 ramps up with generator 1 providing balancing adjustments, the transmission network becomes strained and eventually fails to supply the increasing load.

A continuation power flow [36], [37] provides valuable insight in this type of scenario. A loading parameter incrementally increases the nominal power requested by load 2 until the maximum value of this parameter is identified. LTC taps are allowed to vary smoothly during this process to provide voltage regulation and the active power limits on generator 1 are ignored. Assuming nominal voltages, load 1 is set to $30 + \mathbf{j}18$ pu, and load 2 starts at 32 pu. The system behaviour as load 2 increases is shown in Figure 13.

The maximum nominal power of load 2 is 34.98 pu and is clearly evidenced by the vertical slope on the voltage curves in Figure 13a. At this condition, both LTCs are at their respective lower limits in Figure 13b and generators 2 and 3 are both producing their maximum reactive power in Figure 13d. Figure 13c shows that the maximum active power which is actually delivered to load 2 is only 33.97 pu and occurs when the nominal demand is 34.19 pu.

The first indication that the system is strained occurs as generator 3 reaches its reactive power limit. As its terminal voltage begins to drop, a low voltage alarm signals that MPC should begin to operate. Subsequent warning signs include LTC 2 reaching its lower tap limit, closely followed by

TABLE IV
MPC OBJECTIVE COEFFICIENTS FOR RAMPING BPA LOAD

Term	MPC
p_{Gn}	1
Δp_{Gn}	0.1
q_{Gn}	0.1
p_{Dn}^{red}	1,000
V_n^+, V_n^-	100
V_{ij}^{ref}	100
a_{ij}	0.01

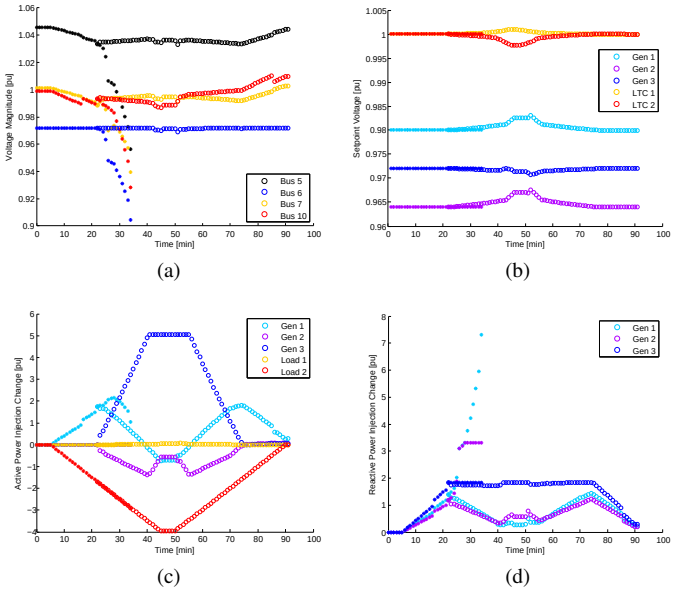

Fig. 14. Conditions of the BPA network with one of the high voltage transmission lines removed and load 2 experiencing a slow ramp. Behaviour with and without MPC intervention are shown by '$\circ$' and '$*$', respectively. Changes in power are with respect to the conditions at time 0.

LTC 1 reaching its limit, and finally, generator 2 reaching its reactive power limit. After this point, system voltages degrade very quickly, and the reactive power output of generator 1 significantly increases.

The behaviour shown in Figure 13 assumes that generator 1 supplies the active power required as load 2 increases. If generation is shifted into the load region, greater loading levels become possible. MPC is able to initiate this type of behaviour to satisfy demand levels that cannot be supplied by generator 1 alone. The objective weights used for MPC in this example are given in Table IV.

Consider similar conditions as those used in the continuation power flow. Load 1 is set to $30 + \mathbf{j}18$ pu, and load 2 increases from 32 pu to 36 pu at a rate of 6 pu/hr. The peak load is sustained for 5 minutes and then ramps back down to its starting level at an equal rate. Generator 1 balances the changes in active power. As was shown in Figure 13, the system will experience voltage collapse as load 2 approaches 35 pu.

Figure 14 shows the system behaviour during the ramp event. At minute 22 with load 2 at 33.7 pu, generator 3 reaches its reactive power limit, triggering a low voltage warning and causing MPC to begin operating. Without intervention, voltages decline in Figure 14a until the power flow eventually fails to converge between minutes 34 and 35 as load 2 reaches 34.9 pu. With MPC intervention, voltage magnitudes remain fairly steady throughout the ramping event. The voltage set-points in Figure 14b also remain fairly constant. Slight adjustments are made during the heaviest demand period from minutes 40 to 55.

MPC begins to shift the active power generation from generators 1 and 2 to generator 3 when it begins operating, as shown in Figure 14c. The inexpensive shift in generation allows it to minimize the more expensive costs of voltage deviations at generator buses. At minute 41, generator 3 reaches its active power limit and generator 2 picks up the power changes during the peak load period. Only a very small amount (< 0.06 pu) of demand response is used during the peak load period. The reactive power needs shown in Figure 14d are also reduced by shifting generation into the load area. Notice though that without MPC intervention, significant reactive power production is required.

The BPA network provides tractable examples of voltage collapse. With relatively few devices, behaviour is easy to identify and useful insights into MPC choices can be discussed. However, the lack of thermal constraints fails to demonstrate the benefits of a control formulation accounting for both transmission and transformer behaviour. Therefore, a case study which incorporates both conditions is presented in the following section.

VI. NORDIC NETWORK

Another test network commonly used in voltage stability studies is the Nordic system [38]. This network is larger than the BPA network with 74 buses, 20 generators, and 22 loads. A diagram summarizing the 400 kV portion of the system is shown in Figure 15. The network is partitioned into four general regions. Generation in the Equivalent and North regions supplies demand in the Central region. The South region is loosely connected to the Central region. The North-Central power transfer occurs over five transmission lines at the 400 kV level. Voltage sensitive loads are connected to the system through tap changing distribution transformers.

A voltage instability event can be initiated by tripping one of the 400 kV lines connecting the North and Central regions. Generators in both regions approach their reactive power limits as LTCs restore the load voltages. Without intervention, transmission voltages eventually drop low enough that a power flow fails to converge.

Thermal (conductor heating) characteristics of transmission lines can be observed in the network behaviour by further weakening the connection between the Central and South regions. Setting the objective coefficients so that generation changes are less expensive in the Equivalent and South regions than in the North and Central regions causes MPC to shift generation from the Equivalent to the South region to relieve the stress on the North-Central transmission corridor and restore voltages. The MPC objective coefficients used in testing are given in Table V.

To test the response of MPC to voltage instability, the system is set to operating point 'A' described in [38]. Loads

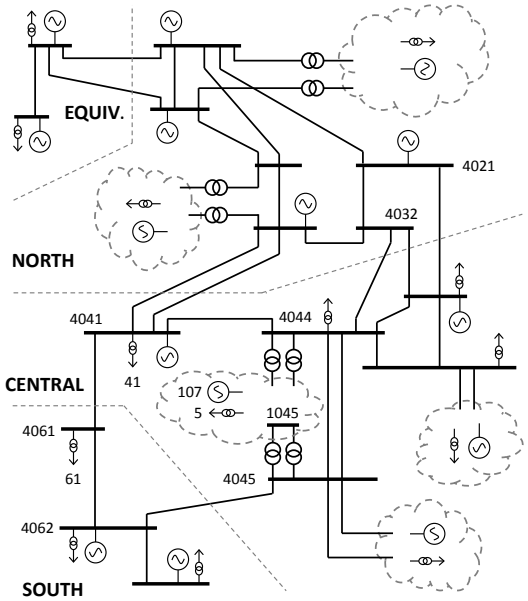

Fig. 15. Summary of the 400 kV portion of the Nordic network adapted from [38]. The primary load centre is the sub-transmission region connected to buses 4044 and 4045. Voltage instability occurs if a transmission line connecting the North and Central regions is lost.

TABLE V
MPC OBJECTIVE COEFFICIENTS FOR NORDIC SYSTEM

Term	MPC
(Equiv./South) p_{Gn}	1
(North/Central) p_{Gn}	100
Δp_{Gn}	0.1
q_{Gn}	0.1
p_{Dn}^{red}	1,000
V_n^+, V_n^-	100
V_{ij}^{ref}	100
a_{ij}	0.01
$\Delta\hat{T}_{ij}$	100

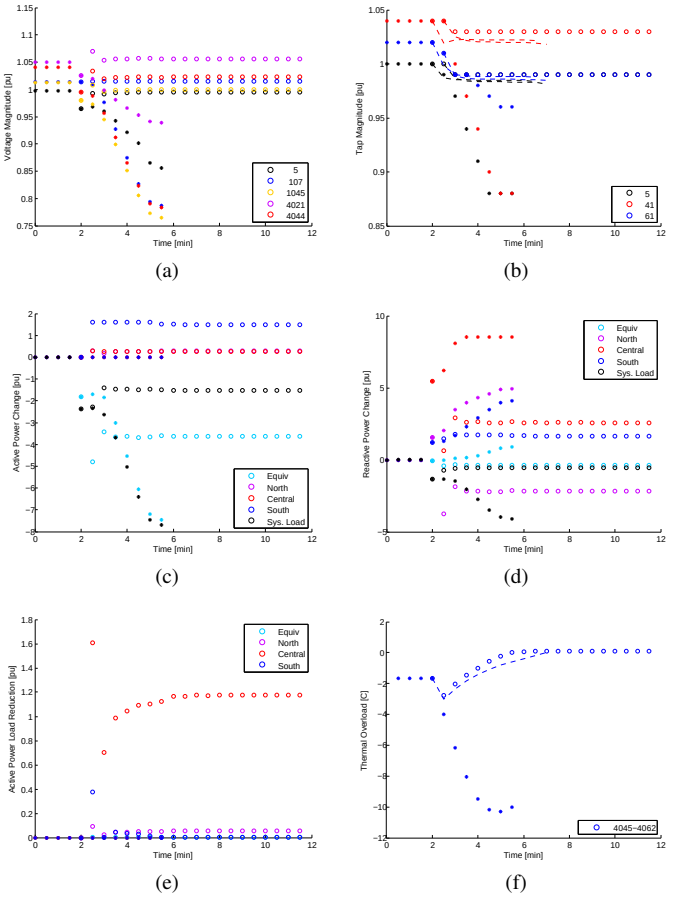

Fig. 16. Conditions of the Nordic test. Behaviour with and without MPC intervention is shown by '$\circ$' and '$*$', respectively. Changes in power are with respect to the conditions at time 0. Dashed curves represent predictions by MPC.

remain at this level during the duration of the test. The Central-South transmission line connecting buses 4045 and 4062 is derated to 335 MVA. The system operates normally for two minutes before a double contingency occurs, and lines 4032-4044 and 4041-4061 are tripped out of service. MPC begins to operate with prediction horizon length $M = 11$ and time-step $T_s = 30$ seconds.

The system behaviour during the test is shown in Figure 16. Conditions when MPC is not operating are denoted by '$*$' markers, and those when MPC is operating are shown by '$\circ$' markers. The slack generator in the Equivalent region accounts for active power changes as LTCs attempt to restore load voltages. This causes voltages to collapse just prior to minute 6. Alternatively, MPC quickly stabilizes voltages by shifting generation from the Equivalent to the South region while respecting the thermal rating of the remaining transmission line connecting the South and Central regions (line 4045-4062).

Several network voltages are shown in Figure 16a. The contingency occurs at minute 2, causing voltages across the network to dip. Without MPC, LTC operation begins to restore the voltage at load bus 5 at time 2:30. However, this increases the reactive power demand and causes generator 107 to drop below its set-point voltage as it reaches its reactive power limit. Transmission and sub-transmission voltages also continue to decline as other generators reach their reactive power limits and load LTCs continue adjusting their taps. Finally, collapse occurs just after time 5:30.

MPC begins operating at minute 2. It predicts the LTC operation and initiates corrective measures to prevent generator voltages from decreasing. This causes the voltage at load bus 5 to almost completely recover by time 2:30. However, the tap change predictions by MPC are larger than the actual changes which occur by time 2:30 due to the discrepancies of the linear transformer model. This produces an overcorrection of transmission voltages at time 2:30. MPC resolves the overcorrection by minute 3 and the system settles to the post-contingency equilibrium between times 3:30 and 6.

The tapping behaviour at several load LTCs is shown in Figure 16b. The predictions of tap behaviour during the first two operations of MPC are shown by the dashed curves. The discrepancy between the predicted and actual behaviour between times 2 and 2:30 is very apparent for the LTC connected to load 41. This device is configured to change its tap in steps of 0.01 pu with an initial fixed delay of 31 seconds

and subsequent fixed delays of 9 seconds. MPC predicts that the tap will decrease by about 0.02 pu by time 2:30. However, the fixed delay prevents any tap changes from occurring by this point. Similar errors occur at other LTCs. The aggregation of these errors causes MPC to select more aggressive control than is actually required during the first period of operation. The predictions at the second operation of MPC better match the actual behaviour and allow MPC to resolve the overcorrection. Despite the initial modeling errors during rapid changes at the beginning of the event, the general trend of tap behaviour predicted by MPC over the horizon approximates the true response and allows MPC to identify useful control actions.

Changes in active and reactive power from the pre-contingency conditions are shown in Figures 16c and 16d, respectively. In both figures, the regional changes in generation and the total change in system load are shown. Without MPC, the slack generator in the Equivalent region tracks changes in load in Figure 16c. MPC shifts generation from the Equivalent region into the South region. The overcorrection in control is balanced by the slack generator at time 2:30 and resolved as time progresses. Figure 16d demonstrates how reactive power requirements are significantly reduced by the controls identified by MPC.

Although load reduction control is expensive, Figure 16e shows that MPC employs it in the Central region. This allows voltage deviation penalties to remain small and satisfies the requirement that any transmission line thermal overloads be removed by the end of the prediction horizon. The aggressive control is also easily seen in this figure at time 2:30. The tap changes predicted within MPC would restore load voltages and load powers. Therefore, MPC employs load shedding to reduce the demand in the Central region. When the tap-induced load restoration predicted by MPC does not materialize, load shedding is reduced over the time interval 2:30 to 3 minutes and then slowly increases to balance thermal overload conditions between the South and Central regions.

The thermal overload on the South-Central transmission interconnection is shown in Figure 16f. The discrepancies in voltage predictions at buses 4045 and 4062 are small enough that the accuracy of the thermal prediction on the transmission line is not significantly affected. Due to high penalties on thermal overloads, MPC respects the thermal limit at the new equilibrium condition. With smaller objective penalties, MPC would allow the thermal overload to settle at about 4 °C. The initial drop in temperature is due to a decrease in load before generation shifts into the South region. When MPC does not operate, the generation pattern remains unchanged and the thermal limit does not present a concern to the system.

VII. Conclusions

Numerous power systems have experienced voltage collapse, typically when the loading is high and/or the system has been weakened through outages. The voltage collapse process often involves excessive tapping of voltage-regulating transformers and exhaustion of reactive power resources. Events leading to collapse can unfold quite quickly, leaving operators with little time to develop and implement effective responses. Model-predictive control (MPC) has been proposed as a corrective control strategy for alleviating voltage collapse. MPC relies on a model of the system that can provide a sufficiently accurate prediction of behaviour over a finite horizon. For voltage-regulating transformers, the model must take into account nonlinear and nonsmooth characteristics that include voltage deadband, time delay, discrete tap steps and tap limits. Even though the proposed model is quite approximate, investigations using two standard test cases suggest that prediction accuracy is sufficient for MPC to successfully prevent voltage collapse.

References

[1] "Modeling of voltage collapse including dynamic phenomena," CIGRE Task Force 38-02-10 Report, 1993.

[2] "Indices predicting voltage collapse including dynamic phenomena," CIGRE Task Force 38.02.11 Report, 1994.

[3] "Criteria and countermeasures for voltage collapse," CIGRE Task Force 38.02.12 Report, 1994.

[4] L. Fink (Editor), "Proceedings: Bulk power system voltage phenomena - voltage stability and security," EPRI Report EL-6183, Potosi, Missouri, January 1989.

[5] ——, "Proceedings: Bulk power system voltage phenomena II - voltage stability and security," ECC/NSF Workshop, Deep Creek Lake, MD, August 1991.

[6] ——, "Proceedings: Bulk power system voltage phenomena III - voltage stability, security and control," ECC/NSF Workshop, Davos, Switzerland, August 1994.

[7] S. K. Chang, F. Albuyeh, M. L. Gilles, G. E. Marks, and K. Kato, "Optimal real-time voltage control," *IEEE Transactions on Power Systems*, vol. 5, no. 3, pp. 750–758, Aug 1990.

[8] S. Corsi, M. Pozzi, C. Sabelli, and A. Serrani, "The coordinated automatic voltage control of the Italian transmission grid–Part I: Reasons of the choice and overview of the consolidated hierarchical system," *IEEE Transactions on Power Systems*, vol. 19, no. 4, pp. 1723–1732, November 2004.

[9] H. Vu, P. Pruvot, C. Launay, and Y. Harmand, "An improved voltage control on large-scale power system," *IEEE Transactions on Power Systems*, vol. 11, no. 3, pp. 1295–1303, Aug 1996.

[10] D. S. Popovic, V. A. Levi, and Z. A. Gorecan, "Co-ordination of emergency secondary-voltage control and load shedding to prevent voltage instability," *IEE Proceedings - Generation, Transmission and Distribution*, vol. 144, no. 3, pp. 293–300, May 1997.

[11] P. Ristanovic, "Control applications of optimal power flow in EMS," *IEEE Transactions on Power Systems*, vol. 12, no. 1, pp. 451–455, Feb 1997.

[12] X. Wang, G. C. Ejebe, J. Tong, and J. G. Waight, "Preventive/corrective control for voltage stability using direct interior point method," *IEEE Transactions on Power Systems*, vol. 13, no. 3, pp. 878–883, Aug 1998.

[13] E. F. Camacho and C. Bordons, *Model Predictive Control*, 2nd ed. London, UK: Springer-Verlag, 2007.

[14] J. B. Rawlings, "Tutorial overview of model predictive control," *IEEE Control Systems*, vol. 20, no. 3, pp. 38–52, Jun 2000.

[15] M. Larsson, D. Hill, and G. Olsson, "Emergency voltage control using search and predictive control," *International Journal of Electrical Power and Energy Systems*, vol. 24, no. 2, pp. 121 – 130, 2002.

[16] M. Larsson and D. Karlsson, "Coordinated system protection scheme against voltage collapse using heuristic search and predictive control," *IEEE Transactions on Power Systems*, vol. 18, no. 3, pp. 1001–1006, Aug 2003.

[17] M. Larsson, "A model-predictive approach to emergency voltage control in electrical power systems," in *2004 43rd IEEE Conference on Decision and Control (CDC)*, vol. 2, Dec 2004, pp. 2016–2022 Vol.2.

[18] I. A. Hiskens and M. A. Pai, "Trajectory sensitivity analysis of hybrid systems," *IEEE Transactions on Circuits and Systems I: Fundamental Theory and Applications*, vol. 47, no. 2, pp. 204–220, Feb 2000.

[19] M. Zima, P. Korba, and G. Andersson, "Power systems voltage emergency control approach using trajectory sensitivities," in *Proceedings of 2003 IEEE Conference on Control Applications, 2003. CCA 2003.*, vol. 1, June 2003, pp. 189–194 vol.1.

[20] M. Zima and G. Andersson, "Model predictive control employing trajectory sensitivities for power systems applications," in *Proceedings of the 44th IEEE Conference on Decision and Control*, Dec 2005, pp. 4452–4456.

[21] I. A. Hiskens and B. Gong, "MPC-based load shedding for voltage stability enhancement," in *Proceedings of the 44th IEEE Conference on Decision and Control*, Dec 2005, pp. 4463–4468.

[22] A. G. Beccuti, T. Demiray, M. Zima, G. Andersson, and M. Morari, "Comparative assessment of prediction models in voltage control," in *2007 IEEE Lausanne Power Tech*, July 2007, pp. 1021–1026.

[23] L. Jin, R. Kumar, and N. Elia, "Model predictive control-based real-time power system protection schemes," *IEEE Transactions on Power Systems*, vol. 25, no. 2, pp. 988–998, May 2010.

[24] M. Glavic, M. Hajian, W. Rosehart, and T. V. Cutsem, "Receding-horizon multi-step optimization to correct nonviable or unstable transmission voltages," *IEEE Transactions on Power Systems*, vol. 26, no. 3, pp. 1641–1650, Aug 2011.

[25] M. Glavic and T. van Cutsem, "Some reflections on model predictive control of transmission voltages," in *2006 38th North American Power Symposium*, Sept 2006, pp. 625–632.

[26] M. Hajian, W. Rosehart, M. Glavic, H. Zareipour, and T. V. Cutsem, "Linearized power flow equations based predictive control of transmission voltages," in *2013 46th Hawaii International Conference on System Sciences*, Jan 2013, pp. 2298–2304.

[27] S. R. Islam, K. M. Muttaqi, and D. Sutanto, "Multi-agent receding horizon control with neighbour-to-neighbour communication for prevention of voltage collapse in a multi-area power system," *IET Generation, Transmission Distribution*, vol. 8, no. 9, pp. 1604–1615, Sept 2014.

[28] C. Taylor, *Power System Voltage Stability*. McGraw-Hill, 1994.

[29] T. van Cutsem and C. Vournas, *Voltage Stability of Electric Power Systems*. Norwell, MA: Kluwer Academic, 1998.

[30] *PJM Manual 12: Balancing Operations*, 35th ed., PJM, Aug 2016.

[31] *Manual 12: Transmission and Dispatching Operations Manual*, 3rd ed., New York Independent System Operator, Feb 2016.

[32] *Manual 15: Emergency Operations Manual*, 7th ed., New York Independent System Operator, Apr 2016.

[33] M. Almassalkhi, "Optimization and model-predictive control for overload mitigation in resilient power systems," Ph.D. dissertation, University of Michigan, 2013.

[34] I. Hiskens and D. Hill, "Dynamic interaction between tapping transformers," in *11th Power Systems Computation Conference*, 1993.

[35] I. Hiskens and C. McLean, "SVC behaviour under voltage collapse conditions," *IEEE Transactions on Power Systems*, vol. 7, no. 3, pp. 1078–1087, August 1992.

[36] G. Price, "A generalized circle diagram approach for global analysis of transmission system performance," *IEEE Transactions on Power Apparatus and Systems*, vol. PAS-103, no. 10, pp. 2881–2890, October 1984.

[37] I. Hiskens and R. Davy, "Exploring the power flow solution space boundary," *IEEE Transactions on Power Systems*, vol. 16, no. 3, pp. 389–395, August 2001.

[38] T. van Cutsem *et al.*, "Test systems for voltage stability analysis and security assessment," IEEE Power and Energy Society, Tech. Rep. 19, Aug 2015.